Journal of Photochemistry and Photobiology A: Chemistry 210 (2010) 115–124

Contents lists available at ScienceDirect

Journal of Photochemistry and Photobiology A: Chemistry

journal homepage: www.elsevier.com/locate/jphotochem

# Probing solute–solvent hydrogen bonding with fluorescent water-soluble curcuminoids

Monica Caselli[a], Erika Ferrari[a], Carol Imbriano[b], Francesca Pignedoli[a], Monica Saladini[a], Glauco Ponterini[a,*]

[a] Dipartimento di Chimica, Università di Modena e Reggio Emilia, via Campi 183, 41100 Modena, Italy
[b] Dipartimento di Biologia Animale, Università di Modena e Reggio Emilia, via Campi 213/D, 41100 Modena, Italy

ARTICLE INFO

*Article history:*
Received 30 November 2009
Received in revised form 8 January 2010
Accepted 13 January 2010
Available online 25 January 2010

*PACS:*
31.50.Df (excited states atomic and molecular)
33.50.Dq (fluorescence of molecules)
33.15.Fm (hydrogen bonding in molecules)
31.70.Dk (solvent effects in atomic and molecular interactions)

*Keywords:*
Curcuminoid
Photophysics
Solvent effects
Hydrogen bonding
Radiationless transition

ABSTRACT

Glycosylated water-soluble curcuminoids (C1–C3, first scheme of this article) differing in the 3,3′-ring substituents (–OH, $-OCH_3$ and H) equilibrate between the di-keto and the keto–enol forms. The former are well observable in the absorption spectra in water, but their emissions are always negligible. The keto–enol forms of C1–C3 exhibit a broad range of fluorescence quantum yields in different solvents, organic and water: formation of solute–solvent hydrogen bonds through the 3,3′-ring substituents may change the radiationless $S_1$-state decay constant by up to a factor 200. Such a fluorescence quenching mechanism is extremely efficient in water and, for C1, in accepting organic media. On the contrary, no effects traceable to intermolecular hydrogen bonds involving the central β-dicarbonyl moiety have been observed. So, fluorescence of these curcuminoids may probe the hydrogen bonding ability, particularly as acceptor, of their microenvironments, including hydrophilic/hydrophobic domains in complex biological systems. Interaction of C1 and C2 with bovine serum albumin results in emission enhancements inverse to the quantum yields of the curcuminoids in water. The observations support the idea that, although the curcuminoid microenvironment within its complex with the protein is less polar and hydrogen bonding than water itself, residual water/ligand hydrogen bonds are active in enhancing radiationless transitions. Finally, fluorescence confocal images of HCT116 cells treated with C1–C3 suggest the apparently small structural differences to affect, besides their fluorescence behaviour, their interactions and fate within living cells.



## 1. Introduction

The polyphenol curcumin, the active ingredient in the traditional herbal remedy and dietary spice turmeric (Curcuma longa) [1], features a wide range of beneficial properties, including anti-inflammatory, antioxidant, chemopreventive and chemotherapeutic activity (see Ref. [2] for a recent updated bibliography). However, its clinical use is severely limited by its extremely low bioavailability, which is a consequence of poor solubility and instability in aqueous solution, in particular at alkaline pH [3,4]. To improve curcumin solubility in water, conjugation with nucleosides [5] and biopolymers [6] has been carried out. We have recently synthesized and characterized a series of water-soluble curcumin glycosyl derivatives (Scheme 1), also able to act as metal-chelating agents [7,8]. These molecules were found to be cytotoxic towards human ovarian carcinoma cells with good selectivity versus non-cancer cells [9].

Within the bio-pharmacological applications of curcumin, its electronic absorption and fluorescence properties (spectra, quantum yield, lifetime, anisotropy) are of great relevance for both analytical applications (e.g., the characterization of complexation equilibria) and molecular-scale functional and structural studies. The variations in UV–vis, fluorescence and circular dichroism properties, particularly in fluorescence intensity, have provided information on the interaction of curcumin with proteins such as human serum albumin [10–13], bovine serum albumin [12,14], egg albumin [12], and with phosphatidylcholine liposomes which are curcumin carriers in living cells [11]. Curcumin [15–17] and, though to a much lower extent, its analogue lacking the substituents at the aromatic rings [2] exhibit a marked solvent dependence of the electronic absorption and emission spectra as well as of the photophysics and photochemistry. Both a solvent-dependent keto/enol tautomerism of the central unsaturated β-dicarbonyl moiety and *cis*/*trans* isomerism of the chromophoric carbon-atom chain might contribute to the complex behaviour [16,18]. Strong six-membered-ring intramolecular hydrogen bonding makes the *cis* keto–enol form in Scheme 1 the most stable one for β-dicarbonyls unsubstituted at the central C atoms in low-polarity solvents [18],

* Corresponding author. Tel.: +39 059 2055084; fax: +39 059 373543.
*E-mail address:* glauco.ponterini@unimore.it (G. Ponterini).

1010-6030/$ – see front matter © 2010 Elsevier B.V. All rights reserved.
doi:10.1016/j.jphotochem.2010.01.008

and for curcumin in the solid state [19]. However, strong perturbation, if not disruption, of this intramolecular hydrogen bond takes place for β-dicarbonyls in polar solvents: while *trans* or *cis* di-keto forms are usually stabilized by an increase in polarity and, to a smaller extent, in hydrogen-bond donating ability of solvents, the enol forms are believed to be stabilized by hydrogen-bond accepting solvents (see [18] and references quoted therein). Formation of hydrogen-bonded complexes of curcuminoids with methanol [20] and water [21] has been observed in the crystal state. Evidence based on NMR [16,22–24] and UV–vis [24,25] spectra indicate curcumin to assume preferably the keto–enol form in organic solvents, both protic and aprotic, and theoretical work leads to the same conclusion for curcumin in the gas phase and in water [24,26].

The curcumin fluorosolvatochromism was mainly attributed to solute–solvent dipolar interactions and a significant charge-transfer character of the $S_0$–$S_1$ transition, with some specific effects – intermolecular hydrogen bonding with protic solvents and π-bonding with aromatic ones – playing some role [16]. As for the decay kinetics of the lowest excited singlet state ($S_1$), this was always fast but, again, showed some solvent modulation. Different explanations have been given. In an earlier paper [16] biexponential decays were observed, with a dominant shorter-lived component (lifetimes between 52 and 348 ps) in all solvents except benzene, and a much weaker longer-lived one (lifetimes between 239 and 1150 ps). The latter was attributed to the di-keto tautomer and the former to the dominant keto–enol one, whose $S_1$–$S_0$ internal conversion would be accelerated by formation of intramolecular hydrogen bonds in hydrocarbons and by solute–solvent hydrogen bonds in polar organic solvents. The two emissions were assumed to spectrally overlap. A more detailed analysis of curcumin $S_1$ decay kinetics [2,17] has confirmed that internal conversion is the dominant decay path, but has revealed a role of the hydrogen bonding abilities of solvents in modulating such kinetics. An ultrafast ($10^{11}$ $s^{-1}$) excited-state intramolecular proton transfer (ESIPT) between the hydroxyl- and the carbonyl group of the hydrogen-bonded cis-enol isomer of curcumin, followed by radiationless excited-tautomer decay, was claimed to explain the shortest and predominant component (57 ps) in cyclohexane, while the intermediate component (256 ps) was attributed to an excited-state photoisomerization channel. Strong perturbation, possibly breaking, of the intramolecular hydrogen bond was believed to occur in protic solvents; the biexponential decays in these media (117–708 ps) were attributed to solute-to-solvent charge or energy transfer (faster component) and an intramolecular ESIPT triggered by a relatively slow de-solvation step occurring either in the *trans* or in the open *cis* keto–enol forms. The latter was proposed to account for the slower, single-exponential decays (467–702 ps) observed in non-hydrogen-bonding, polar solvents [2,17]. Very similar explanations were proposed to interpret the photophysical behaviour of a curcuminoid lacking both the aromatic hydroxyl and methoxy substituents [2]. The larger complexity exhibited by this compound with respect to curcumin was tentatively accounted for by assuming that, in all solvents, it exists mainly as a solvent-sensitive equilibrium mixture of two *cis* keto–enol conformers that decay by different ESIPT paths characterized by slightly different rates [2]. Support to the occurrence of radiationless decays of curcumin through ESIPT paths has been provided in a recent femtosecond fluorescence upconversion study [27]. Here, the fluorescence decay of curcumin in methanol and ethylene glycol was found to be double-exponential: a fast component (12 and 20 ps, respectively), insensitive to solvent deuteration, correlated with a time-shift of emission and was assigned to solvation dynamics triggered by the change in electric dipole moment upon $S_0$–$S_1$ excitation; the slower component (70 and 105 ps, respectively) exhibited a marked deuteration effect (following a slow solute–solvent H-D exchange) and was essentially viscosity independent. On this basis, it was assigned to an intramolecular excited-state hydrogen-atom transfer occurring in these alcohols and in chloroform (130 ps) on a timescale much longer than that of the same process in 3-hydroxyflavone (240 fs) [28]. Apparently, throughout the literature concerning curcumin, the hydrogen bonds relevant to the photophysical behaviours were always assumed to involve the curcuminoid di-keto or keto–enol central moiety; in no case was the possibility of a direct involvement of the OH($OCH_3$) ring substituents taken into account.

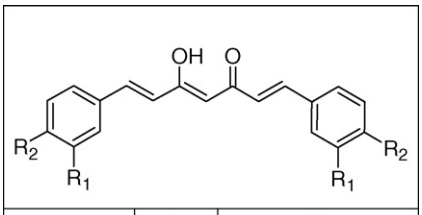


| | $R_1$ | $R_2$ |
|---|---|---|
| **Curcumin** | $OCH_3$ | OH |
| **C1** | OH | 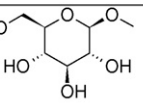 (GlcO-) |
| **C2** | $OCH_3$ | GlcO- |
| **C3** | H | GlcO- |

**Scheme 1.**

Because of the bio-pharmacological relevance of curcuminoids, in this paper we wish to reanalyze their electronic spectra and photophysics in polar solvents, including water, with the purpose of providing evidence for the decisive role of inter-, rather than intramolecular hydrogen bonds in modulating their fluorescence emission quantum yields in biologically relevant microenvironments. As has been recently pointed out [2], with curcumin derivatives substituents at the aromatic rings are expected to affect the π-electron chromophoric systems as well as the hydrogen bonding propensities, both intra- and intermolecular. We have investigated three curcuminoids, C1–C3 in Scheme 1, which differ only in the 3,3′-substituents at the phenyl rings. It will be clear, however, that changing from the hydroxylic substitution (C1, both donor and acceptor in intermolecular hydrogen bonds) to the methoxy one (C2, acceptor only) to no substitution (C3) drastically and consistently changes the pattern of the fluorescence quantum yields in solvents such as water, methanol and glycerol (hydrogen bond donors and acceptors), dimethylsulfoxide (DMSO, good acceptor) and acetonitrile (very weak acceptor). To test the effects of more biologically significant microenvironments on the fluorescence behaviour of the three compounds, their binding to bovine serum albumin (BSA) was monitored using both curcuminoid and intrinsic protein fluorescence emissions. Finally, C1–C3 emission was exploited to investigate their distribution within HCT116 cells by confocal fluorescence imaging.

## 2. Materials and methods

### 2.1. Chemicals

All reagents and chemicals were from Sigma–Aldrich and were used without further purification. Glycosyl curcuminoids (C1–C3) were synthesized as previously reported [9] and their purity was checked to be >95% by means of NMR and combustion analysis. Freshly prepared solutions were employed in all cases.

### 2.2. Absorption spectra

UV–vis absorption measurements were performed using either a Jasco V-570 or a Varian Cary 100 spectrophotometer. Oscillator strengths of the lowest-energy bands were determined in a protic and an aprotic solvents, methanol and DMSO, as $f = 4.32 \times 10^{-9} n^{-1} \int \varepsilon(\bar{\nu}) d\bar{\nu}$ [29], where n is the solvent refractive index; the extinction coefficients, $\varepsilon$, were obtained from two independent samples and the integration was performed between 300 and 400 nm (25,000 and 33,333 $cm^{-1}$).

### 2.3. Steady-state and time-resolved fluorescence measurements

Fluorescence experiments were carried out on a Spex Jobin-Yvon Fluoromax-3 spectrofluorometer. Spectra were corrected for the instrumental spectral sensitivity. Fluorescence quantum yields ($\Phi_F$) were determined relative to fluorescein in 0.1 M NaOH ($\Phi_F = 0.95$ [30]). The fluorescence lifetimes ($\tau_F$) of curcuminoids C1–C3 in methanol, acetonitrile and glycerol were measured with an IBH System 5000 single photon counting apparatus having a time resolution of about 0.5 ns after deconvolution. The fluorescence decay functions, expressed as the sum of exponential decays, were deconvoluted from the measured time profiles using a combined linear and non-linear iterative reconvolution method based on the minimization of the $\chi^2$ parameter. The goodness of fit was evaluated on the basis of the value of $\chi^2$ ($\leq$1.2) and of the distribution of residuals. The fluorescence decays of curcuminoids in methanol and acetonitrile were fitted by single exponential functions, whereas in glycerol the decays were biexponentials with a minor longer-time component. Radiationless $S_1$-decay rate constants were calculated as $k_{nr} = \tau_F^{-1}(1 - \Phi_F)$, whenever the lifetime, $\tau_F$, was available, and as $k_{nr} = k_r(\Phi_F^{-1} - 1)$, assuming $k_r = 2.2 \times 10^8\ s^{-1}$, in the other cases. All measurements were performed at room temperature (22 ± 5 °C).

### 2.4. Data analysis of curcuminoid/BSA titrations

For the reasons described in Section 3.2, a Benesi-Hildebrand-type approach (Eq. B14 in Ref. [31]):

$$\frac{I_0}{I - I_0} = \frac{\alpha}{K[\mathrm{M}]} + \alpha \quad (1)$$

was used to analyze the fluorescence intensities of curcuminoids C1 and C2 upon titration with BSA. Here $I$ and $I_0$ are the fluorescence intensities at a given pair of excitation and emission wavelengths in the presence and absence of BSA, $K$ is the complex association equilibrium constant and $\alpha$ is a combination of coefficients that relate the emission intensities of the free and bound ligand to their concentrations. The assumptions here are that 1:1 complexes are formed and that [M], the concentration of unbound macromolecule, can be replaced by its total concentration; this is true when $K{\cdot}[C]_t \ll 1$, $[C]_t$ being the total curcuminoid concentration which, according to an additional usually tacit assumption, should be kept unchanged during the titration. We took care to make both latter assumptions true, leaving a check of the first one to the assessment of the quality of data fitting. Inner filter effects on BSA emission intensities, measured in protein titrations with the three curcuminoids, were approximately corrected as follows [32]:

$$I_{corr} = I_{meas} 10^{((A_{290} + A_{343})/2)} \quad (2)$$

where $A$ are the total absorbances at the excitation and emission wavelengths and, for both the incoming excitation beam and the outcoming emitted one, an average path length half the total cuvette width is assumed. The corrected data were then fitted to Eq. (3) [31]:

$$I = I_0 + \frac{I_{lim} - I_0}{2} \left\{ 1 + \frac{[\mathrm{BSA}]}{[C]} + \frac{1}{K[C]} - \left[ \left( 1 + \frac{[\mathrm{BSA}]}{[C]} + \frac{1}{K[C]} \right)^2 - 4\frac{[\mathrm{BSA}]}{[C]} \right]^{1/2} \right\} \quad (3)$$

where $I_0$ is the protein fluorescence intensity with no added curcuminoid ($C$) and $I_{lim}$, the intensity at full BSA complexation, was both obtained from visual data extrapolation and left as a floating parameter in the non-linear least squares analysis. This was performed with the Microcal Origin 6.0 program.

### 2.5. Fluorescence confocal microscopy imaging of curcuminoids in cells

The HCT116 cell line was generously provided by Bert Vogelstein (Johns Hopkins University School of Medicine, Baltimore, MD). The cells were derived from a human colorectal carcinoma and were cultured in IMDM medium supplemented with 10% FCS (fetal calf serum). The curcuminoids were added to the cell medium at a 20 μM concentration for 24 h. The culture medium (3 ml) was acidified with 6N HCl (1:1 (v/v)) and vortexed for 30 s. Following addition of 3 ml of extracting buffer (ethyl acetate and isopropanol 9:1 (v/v)), samples were each vortexed again and then shaken in the Orbited shaker (at 100 rpm) for 15 min. After centrifugation at 18000 rpm for 20 min, the upper organic layer was filtered through a membrane filter (0.22 μm) and directed to UV–vis analysis. The cell pellets were resuspended in the RIPA buffer (20 mM Tris/HCl at pH 8.0, 137 mM NaCl, 10% of glycerol, 5 mM EDTA, 1 mM phenylmethyl-sulfonyl fluoride, 1.5 mg of leupeptin, and protease inhibitor cocktail) and the cell–liquid extraction was carried out. The cell extracts were cleared by centrifugation at 18,000 rpm for 15 min and acidified by 6N HCl (1:1 (v/v)) and vortexed for 30 s. Then the same extracting procedure as for culture medium was performed. For confocal microscopy imaging, 300,000 cells were seeded on coverslips the day before drugs treatment. After drugs incubation, cells were washed twice in PBS 1× at room temperature, fixed in cold methanol/acetone for 2′. After three washes in PBS 1×, monolayers were mounted with Vectashield and examined by Leica DM IRE2 with multiband scan Leica TCS SP2 with AOBS.

## 3. Results

### 3.1. Solvent dependence of electronic spectra and photophysics

The electronic absorption spectra of curcuminoids C1–C3 were measured in five polar solvents (the three compounds are insoluble in hydrocarbons). The spectra of C1 are shown in Fig. 1. The neutral forms prevail in water at pH 3 and in the organic solvents and feature an intense lowest-energy band with maxima between 400 and 425 nm (details are in Table 1). This is quite similar, in both position, shape and intensity, for the three compounds in a given solvent and, conversely, for each compound in different solvents: both the different 3,3′ substituents and solvent proticity cause but a small perturbation of the chromophoric π-electron system. Our measured oscillator strengths, which are between 0.65 and 0.78, are about half the values, around 1.5, calculated for gas-phase curcumin or its unsubstituted chromophore [24,25,33]. However, our maximum extinction coefficients, given in Table 1, agree with the experimental one of free curcumin in water, 42,000 [34] or around 40,000 $M^{-1}\ cm^{-1}$ [11].

Additional absorption bands are found for C1–C3 in water between 280 and 380 nm (shown in Fig. 1 for C1), most intense for C3 ($\lambda_{max}$ = 327 nm). Dilution tests proved that such bands were not attributable to aggregation. They might be due to keto–enol isomers in the *trans* or the 'open' *cis* conformations, likely stabilized in such a strongly hydrogen-bonding solvent [2,17]. However,

**Table 1**
Spectroscopic and photophysical data of C1–C3. $\lambda^{max}_{abs/fluo}$ = absorption/fluorescence maxima; $\varepsilon_{max}$ = maximum molar extinction coefficients; $f$ = oscillator strengths; $\Phi_F$ = fluorescence quantum yields; $\tau_F$ = fluorescence lifetimes, written between parentheses when lower than the estimated instrumental resolution, 0.5 ns; $k_{r/nr}$ = radiative/radiationless decay rate constants: $k_r = \Phi_F\tau_F^{-1}$, $k_{nr} = \tau_F^{-1}(1-\Phi_F)$, written between parenthesis when calculated with lifetimes lower than the instrumental resolution, 0.5 ns. Values in italics are estimated as $k_{nr} = k_r(\Phi_F^{-1} - 1)$, assuming $k_r = 2.2 \times 10^8\ s^{-1}$ in all cases. DMSO = dimethylsulfoxide; BSA = bovine serum albumin in 0.1 M Tris buffer.

| Solvent | Curcuminoid | $\lambda^{max}_{abs}$/nm, $\varepsilon_{max}$/$M^{-1}$ $cm^{-1}$, $f$ | $\lambda^{max}_{flu}$/nm | Stokes shift/$cm^{-1}$ | $\Phi_F$ | $\tau_F$/ns | $k_r/10^8\ s^{-1}$ | $k_{nr}/10^9\ s^{-1}$ |
|---|---|---|---|---|---|---|---|---|
| | C1 | 413 | 505 | 4700 | 0.0006 | | | *366* |
| $H_2O$, pH 3 | C2 | 413 | 543 | 5800 | 0.006 | | | *36* |
| | C3 | 403 | 512 | 5300 | 0.13 | | | *1.5* |
| | C1 | 412.5, 41,000, 0.78 | 501 | 4600 | 0.0055 | <0.50 (0.12) | >0.11 (0.5) | >2.0 (8.2), *40* |
| $CH_3OH$ | C2 | 413, 31,000, 0.67 | 526 | 5200 | 0.11 | 0.54 | 2.0 | 1.6 |
| | C3 | 405, 40,000, 0.78 | 496 | 4530 | 0.11 | 0.62 | 1.8 | 1.4 |
| | C1 | 424, 41,800, 0.78 | 502 | 3700 | 0.007 | | | *31* |
| DMSO | C2 | 424, 29,000, 0.65 | 511 | 4000 | 0.12 | | | *1.6* |
| | C3 | 416, 37,000, 0.70 | 490 | 3630 | 0.10 | | | *2.0* |
| | C1 | 424 | 504 | 3740 | 0.045 | <0.50 (0.31), 5.2[a] | >0.9 (1.5) | >1.9 (3.1), *4.7* |
| Glycerol | C2 | 421.5 | 523 | 4600 | 0.13 | 0.61, 4.8[a] | 2.1 | 1.4 |
| | C3 | 413 | 504 | 4370 | 0.18 | 0.74, 3.9[a] | 2.4 | 1.1 |
| | C1 | 408 | 502 | 4600 | 0.09 | <0.50 (0.41) | >1.8 (2.2) | >1.8 (2.2), *2.9* |
| $CH_3CN$ | C2 | 412 | 502.5 | 4370 | 0.18 | 0.67 | 2.7 | 1.2 |
| | C3 | 405.5 | 482 | 3900 | 0.07 | <0.50 (0.29) | >1.4 (2.4) | >1.9 (3.2), *2.9* |
| | C1 | | 479 | | ~0.01 | <0.50 (0.41) | >1.8 (2.2) | >1.8 (2.2), *2.9* |
| BSA | C2 | | 515 | | ~0.01 | 0.67 | 2.7 | 1.2 |
| | C3 | | 511 | | ~0.1 | <0.50 (0.29) | >1.4 (2.4) | >1.9 (3.2), *2.9* |

[a] Decays were biexponential with a minor longer-time component (relative amplitude ≤5%).

such forms have never been found as stable minima in gas-phase structural theoretical studies and no calculations of their absorption spectra is, consequently, available [24–26,33]. We tentatively assign them to the di-keto isomers, likely in the *trans* conformation [26], on the following circumstantial evidence: (i) these forms are non-planar and, consistently, their lowest-energy absorption bands are found to the blue of the corresponding keto–enol isomer bands

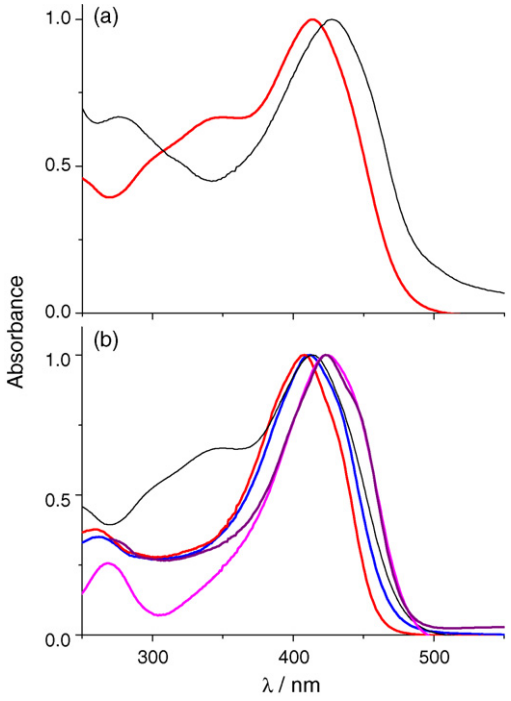


**Fig. 1.** UV–vis absorption spectra of C1 in: (a) water at pH 3 (red) and pH 12 (black); (b) water at pH 3 (black), methanol (blue), DMSO (purple), glycerol (magenta) and acetonitrile (red). Spectra normalized at maxima for ease of comparison. (For interpretation of the references to colour in this figure legend, the reader is referred to the web version of the article.)

[24,25,33]. For the unsubstituted curcumin chromophore in the gas-phase the calculated energy differences between the intense colour band of the keto–enol form (maximum at 419 nm) and the first (389 nm) and the second (373 nm) moderately intense bands of the possibly, di-keto form are, respectively, 1840 and 2940 $cm^{-1}$ [25], somewhat smaller than our experimental differences between the two bands, about 4800, 4400 and 5600 $cm^{-1}$ for C1, C2 and C3 in water. However, calculation of the HOMO–LUMO energy difference of curcumin in this solvent yielded a value for the *anti* di-keto form higher by 3600 $cm^{-1}$ than for the *cis* keto–enol one, more consistent with our experimental findings [26]; (ii) the di-keto isomers of β-dicarbonyls [18] and of unsubstituted curcumin [2] are thought to be stabilized, relative to the keto–enol ones, by an increase in polarity and a decrease in molecular size of the solvent.

Upon excitation within the lowest-energy absorption bands of the keto–enol isomers, single-band, unstructured fluorescence emissions are observed in all examined solvents (Fig. 2). The excitation spectrum of C1 in water (Fig. 2a) overlaps the main absorption band but does not include the, possibly, di-keto bands found below 380 nm; a similar behaviour was exhibited by C2 and C3 in water. Indeed, excitation under these bands caused a slight shift of the overall emissions of C1 (−1200 $cm^{-1}$) and C2 (−630 $cm^{-1}$) and no change on C3, thus indicating the forms responsible for these absorptions to feature very weak direct emissions and no efficient excited-state conversion to the keto–enol ones. All compounds show a good absorption/emission mirror relationship and Stokes shifts between, roughly, 3600 and 5800 $cm^{-1}$ (see Table 1 for the spectroscopic details). A much larger 8400 $cm^{-1}$ shift between the normal absorption and the tautomer emission, as well as strongly differing band shapes, were observed with 3-hydroxyflavone, one of the most extensively studied cases of intramolecular ESIPT [35]. In keeping with the conclusions drawn in Refs. [2,17] on curcumin and its unsubstituted derivative, the mentioned features of the fluorescence spectra of C1–C3 strongly point to a dominant emission from the keto–enol forms and, combined with simple energetic considerations (the di-keto isomer is less stable in the ground state, at least in organic solvents, and has a higher $S_0$–$S_1$ excitation energy than the keto–enol one) rule out the possibility, invoked for curcumin [16], that the di-keto forms may contribute to the observed

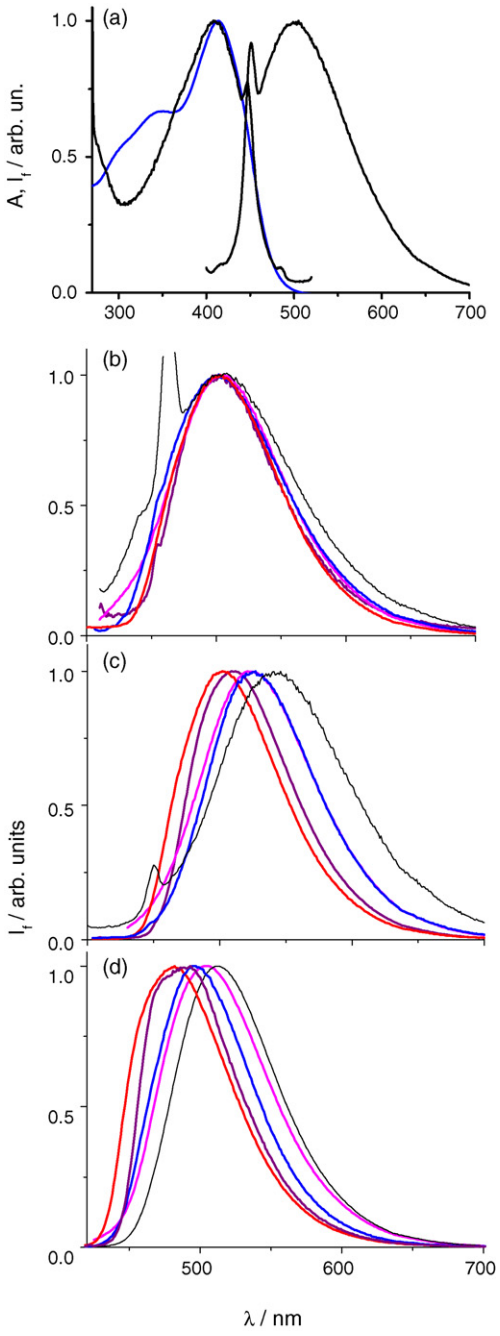


**Fig. 2.** Emission ($I_f$ = fluorescence intensity), excitation and absorption (blue, A = absorbance) spectra of C1 in water at pH 3 (a). Emission spectra of C2 (b), C3 (c) and C4 (d) in water at pH 3 (black), methanol (blue), DMSO (purple), glycerol (magenta) and acetonitrile (red). Spectra normalized at maxima for ease of comparison. (For interpretation of the references to colour in this figure legend, the reader is referred to the web version of the article.)

fluorescence of the three curcuminoids when excited within the main absorption band.

The changes in solvent and in the 3,3′-substitution affect the emission bands to a slightly larger extent than the absorption bands, but the effects remain small since all the maxima of the three compounds fall within a 30 nm range. While the C1 emission is not solvatochromic, those of C2 and C3 shift bathochromically as the solvent is changed from $CH_3CN$ (non-hydrogen bonding) to DMSO (acceptor only), to the alcohols and to water (both donors and acceptors): the emission maxima of the two compounds shift by ca. −1500 and −1200 $cm^{-1}$ from acetonitrile to water. Clearly, given the similarly high polarities of the three organic solvents, it is the formation of solute–solvent hydrogen bonds that stabilizes the $S_1$ state relative to the ground state. That hydrogen bonding lies behind fluorosolvatochromism was found with curcumin too [16], and is consistent with the increase in electron density on the central O atoms calculated in the LUMO relative to the HOMO [24,26]. It is further confirmed by the blurring of the vibronic structure of the absorption band observed, especially for C2 and C3, in protic solvents relative to DMSO (not shown). However, the fact that C1 does not follow the same solvatochromic trend hints at the complexity of the phenomenon, with possible opposite effects canceling out.

Fluorescence quantum yields ($\Phi_F$ in Table 1) exhibit a broad range of values, both in different solvents and with different aromatic ring substituents. Substituent effects are particularly pronounced in water where $\Phi_F$ increases by one order of magnitude from the hydroxy to the methoxy-substituted compounds and by a factor about 200 from the hydroxy to the 4,4′-unsubstituted one. Such changes are due to large changes in radiationless decay rate constants ($k_{nr}$ in Table 1). As mentioned earlier, we obtained the $k_{nr}$ values either directly from measured quantum yields and lifetimes or, in all cases in which the latter were not accessible because of very low emission intensities and very short lifetimes, as $k_{nr} = k_r(\Phi_F^{-1} - 1)$, assuming $k_r$ to hold $2.2 \times 10^8$ $s^{-1}$ for all compounds and solvents. The reliability of this assumption and, within a reasonable confidence range (roughly ±20%), of the thence obtained $k_{nr}$s relies on the consistency of this $k_r$ value with those directly measured for C1–C3 (Table 1) and curcumin [2,16,17] in different solvents, as well as from the similarity of lowest-energy band oscillator strengths of C1–C3 in methanol and DMSO (Table 1). The very large changes in $\Phi_F$ and $k_{nr}$ cannot be attributed to a differential perturbation of the central β-dicarbonyl moiety by the 3,3′-ring substituent change because the similarity of the absorption and emission spectra of the three compounds in all employed solvents tells us that such a differential perturbation is weak. We therefore invoke a direct role of solute/solvent intermolecular hydrogen bonds involving the 3,3′-ring substituents in promoting radiationless deactivation of the $S_1$ states of curcuminoids C1 and C2. More specifically, while the possibility to form water-to-solute hydrogen bonds (compound C2 vs. C3) already opens the way to a fast radiationless deactivation, it is the additional possibility to establish solute-to-water hydrogen bonds (C1 vs. C2) that dramatically speeds up electronic excitation energy thermalisation.

The phenomena leading to fast radiationless decay are much less efficient in organic solvents: relative to its value in water, $k_{nr}$ of C1 decreases by about one order of magnitude in methanol and DMSO, where it is however still around 20 times larger than those of C2 and C3. The latter are instead similar to each other and to those found for all three curcuminoids in acetonitrile (where solute/solvent hydrogen bonding is inactive) and curcumin itself in several solvents except cyclohexane [16,17], i.e., few units times $10^9$ $s^{-1}$. So, solute (C1) to organic solvent (methanol and DMSO) hydrogen bonds involving the 3,3′-OH substituents are still active in promoting a radiationless $S_1$ decay, which remains however much slower than in water. On the contrary, the similarity of the $k_{nr}$ values for C2 and C3 in methanol as well as of those of C1 in methanol and DMSO suggest that methanol-to-solute hydrogen bonds involving the phenyl-ring –$OCH_3$ or –OH substituents are of little relevance in this respect.

The latter conclusion also holds for solvent-to-solute hydrogen bonds possibly involving, as the acceptor, the central dicarbonyl moiety. This is indicated by the similarity of the $k_{nr}$ values of C2 in methanol (that can act as donor), DMSO (acceptor only) and acetonitrile and, most clearly, those of C3 in all solvents. The small solvent effect on the $S_1$ decay of C3, which remains a relatively good fluorophore even in water, somewhat contrasts with the emphasis laid in the literature on the role of intramolecular hydrogen bonds

[16] or ESIPT [2,17] on the radiationless decay of curcumin, when this is combined with the expected dependence of the structure of the central β-dicarbonyl moiety on the medium polarity and proticity [2,16–18]. Our observations indicate that the intramolecular hydrogen bond at the central keto–enol group, while being responsible for the $10^9$–$10^{10}$ $s^{-1}$ $S_1$-state radiationless decay of curcuminoids in organic media, is much less efficient than intermolecular hydrogen bonds involving O atoms of the 3,3′ phenyl substituents in enhancing such a process in hydrogen-bond donating and accepting media, i.e., alcohols and, most pronounced and relevant to the biological applications, water. A strong hint at the crucial role played by these substituents in driving the $S_1$–$S_0$ radiationless decay is provided by the pronounced change in electron density at the $C_3$, $C_{3'}$ atoms between the frontier molecular orbitals of curcumin [24,26]: HOMO-to-LUMO excitation drains electron density from these atoms, and in general from the phenyl rings, to the central C-atom chain. We expect this to result in changes, in $S_1$ relative to $S_0$, of the strengths of hydrogen bonds involving such substituents able to promote fast radiationless decay (vide infra).

We finally observe that, in glycerol, the radiationless decay rates of C2 and C3 are similar to those in methanol ($k_{nr}$ remains, again, of the order of $1 \times 10^9$ $s^{-1}$) but that of C1 is slower by a factor around 10 than that in methanol. Although the difference is likely attributable to the much larger viscosity of glycerol, the mechanistic implication of these observations is however still unclear.

### 3.2. Fluorescence enhancement upon interaction with bovine serum albumin

Following the analysis of the fluorescence properties of C1–C3 in protic/aprotic solvents, we now increase the system complexity and turn our attention to the fluorescence behaviour of these curcuminoids when interacting with proteins. Serum albumins are well-established carriers for a large number of hydrophobic ligands [11,36,37]. Interaction of curcumin with human serum albumin (HSA) has been characterized. According to various experiments (UV–vis absorption, circular dichroism, fluorescence), two binding sites have been found with binding constants differing by one order of magnitude: $2 \times 10^4$ [10] and $1 \times 10^4$ [11], for the first one, $2 \times 10^5$ [10] and $1 \times 10^5$ [11] for the second one. Quite at variance, a single $7.9 \times 10^5$ value has been provided more recently [13]. The disagreement also involves the T-dependence of equilibrium: this was claimed irrelevant in one case [10] but well measurable in a second one ($\Delta H^\circ = -56.9$ kJ mol$^{-1}$, $\Delta S^\circ = -166$ J K$^{-1}$ mol$^{-1}$ [13]). However, the consensus becomes again general over the type of interaction concerned: consistently with the lipophilic nature of curcumin, interaction with HSA occurs through a hydrophobic region (probably domain IIA), about 31 Å from tryptophan 214 [13]. Not surprisingly, quite a similar behaviour has been observed when curcumin interacts with bovine serum albumin: from absorption changes, binding constants around $3 \times 10^4$ and a roughly 1:1.1 stoichiometry were obtained, while evidence of two-site interaction was provided by stopped-flow experiments [14]. Contrary to an earlier observation of an independency of fluorescence intensity of curcumin in the presence of BSA alone, with a one order of magnitude increase only upon surfactant addition [12], a marked (roughly a factor 5) fluorescence enhancement upon complexation with BSA was reported in ref. [14]. However, the quantum yield remained as low as 0.05 thus showing radiationless transitions to be predominant even in the hydrophobic protein microdomains occupied by curcumin.

We wish to see whether the large increase in water solubility achieved for C1–C3 over curcumin by introduction of the gycosyl residues goes along with changes in the interaction with carrier proteins such as albumins. In this contribution, we limit ourselves to the steady-state fluorometric monitoring of the interaction of

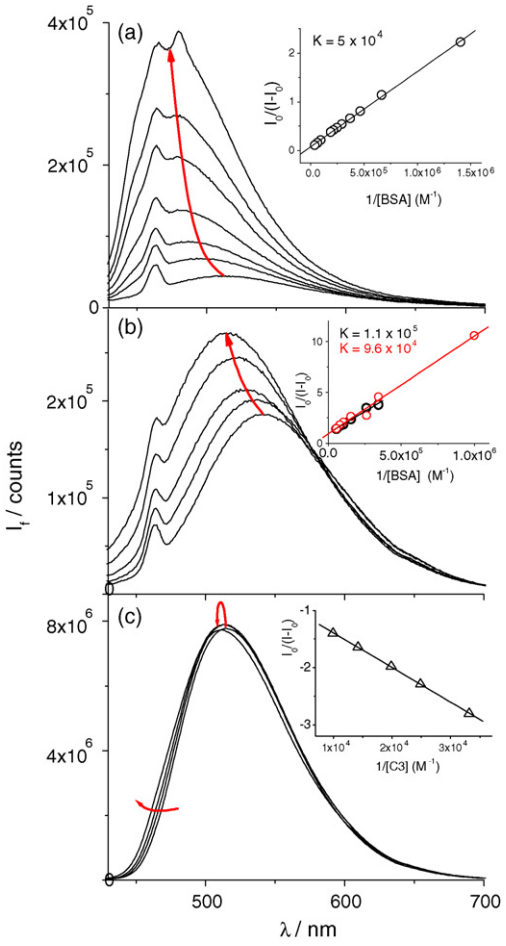


**Fig. 3.** Emission spectra of C1 (a), C2 (b) and C3 (c) as functions of added BSA concentration: 0, 2.5, 5.0, 10, 20, 30, 50 μM for C1; 0, 1.25, 5.0, 15, 30 μM for C2; 0, 1.25, 2.5, 3.75, 5, 10, 15 μM for C3. Curcuminoid concentrations were ca. 5 μM in all cases. Insets: data fitting to Eq. (1) for C1 (a) and C2 (b) emission intensities; fitting to Eq. (1) of BSA emission intensities (c), corrected according to Eq. (2), measured following addition of C3 at concentrations 30, 40, 50, 70 and 100 μM.

curcuminoids C1–C3 with bovine serum albumin (BSA). In contrast with the large absorption changes found for curcumin [14], addition of the protein, up to concentrations of about $2.5 \times 10^{-5}$ M, to $5 \times 10^{-6}$ M solutions of C1–C3 in 0.1 M TRIS buffer, pH 7.4, caused minor (if any) changes in the colour bands of the curcuminoids (data not shown). Only for C3 could we discern a 3 nm red shift, from 410 to 413 nm, of the maximum and a slight but consistent decrease of the 330 nm di-keto band.

Interaction of the three curcuminoids with BSA resulted in different fluorescence behaviours (Fig. 3). C1, that features the lowest quantum yield in water, exhibited the largest fluorescence enhancement – a factor about 10 at $2.5 \times 10^{-5}$ M BSA – and the largest hypsochromic shift of the emission maximum, +1380 cm$^{-1}$, relative to C1 in TRIS buffer. The emission intensity of C2 increased only by about 50%, while the maximum shifted by +950 cm$^{-1}$, relative to C2 in TRIS, at a BSA concentration $1.8 \times 10^{-5}$ M. Finally, C3 exhibited a hardly discernible (within 5%) change in intensity and a very small maximum shift, +150 cm$^{-1}$ relative to C3 in TRIS. So, while the shifts of the emission maxima of C1 and C2 are comparable with those found for curcumin with BSA and HSA (+1250 to 1400 cm$^{-1}$ [11,14]), the C3 emission band position is almost insensitive to protein binding. A rough estimate of the fluorescence quantum yields of C1–C3 interacting with BSA (Table 1) provides values of the order of 1% for the first two compounds and about 10%, again insensitive to the environment, for the third.

So, both fluorosolvatochromic and quantum yield data support the idea, already proposed for curcumin, that C1 and C2 experience a decrease in hydrogen-bonding ability of the environment when interacting with BSA with respect to water. However, the quantum yields of C1 and C2 remain rather low and 10 times lower than that of C3. So, even when these compounds interact with BSA, radiationless transitions, enhanced through hydrogen bonds with residual water molecules, are still two orders of magnitude faster than the radiative $S_1$ decay. Because C3 emission maximum in acetonitrile is shifted by +1330 $cm^{-1}$ relative to water, the lack of emission shift observed with BSA suggests that C3 too, like C1, C2 and curcumin, probes a hydrogen-bonding microenvironment when bound to the protein.

Exploiting the mentioned changes in fluorescence intensities, fluorometric titrations of C1 and C2 with BSA afforded the binding constants at room temperature ($23 \pm 2$ °C). This kind of data analysis may be carried out according to various expressions, whose derivations imply different assumptions and approximations (see, e.g., Refs. [10,11,31,38]). Titrations were carried out up to BSA concentrations around $2 \times 10^{-5}$ M, when the spectral shifts were almost complete but light scattering heavily affected fluorescence which did not show a neat saturating behaviour. So, we could not obtain a limit intensity attributable to full curcumin complexation with BSA, and made use of a simple, Benesi-Hildebrand-type approach (Eq. (1) in Section 2.4). Data were well fitted for C1, while, because of the lower fluorescence enhancement, they were more scattered for C2. In both cases, however, reasonably linear plots were obtained (they are shown in the insets to Fig. 3a and b). Therefore, our data indicate complexation of C1 and C2 by BSA to occur at a single protein site with a simple 1:1 stoichiometry at BSA concentrations lower than ca. $2 \times 10^{-5}$ M. The binding equilibrium constants, obtained as intercept/slope ratios, are $(5 \pm 0.5) \times 10^4$ and $(1 \pm 0.25) \times 10^5$, respectively.

Titration of BSA with the three curcuminoids was also performed. The results of this kind of experiment, although frequently reported in the literature, suffer from serious uncertainties caused by inner filter effects. In our case, the added curcuminoids absorb both at the excitation and at the emission wavelengths of BSA tryptophans, 290 and 343 nm, respectively. In our experiments with C1–C3, the fluorescence intensity decrease of BSA saturated only at such curcuminoid concentrations that the mentioned absorbances were 1–1.5, yielding correction factors (Eq. (2) in Section 2.4) as high as about 10. The measured protein emission intensities decreased similarly with increasing concentrations of the three curcuminoids, with the data obtained with C3 only slightly smaller than those obtained with C1 and C2. However, because of the very large factors, this difference was amplified after correction and the data with the former curcuminoid extrapolated to, roughly, 0 at saturation while those for both latter ones extrapolated to a significantly higher value of ca. 450,000 counts $s^{-1}$. It is tempting to assign a physical significance to this difference, which might suggest that C3 interacts with BSA differently than C1 and C2 and quenches its fluorescence more efficiently at saturation. However, given the very high data corrections, such detailed inferences are probably unreliable and only rough estimations of the binding constants can be obtained from analysis of the corrected data. We have tried to fit them using Eq. (1) in Section 2.4, with [BSA] replaced by the curcuminoid concentrations, [C1–C3]. At variance with the previous case, the assumption that the free curcuminoid concentration can be replaced by its total concentration (see Section 2.4) only holds for few, high concentration points. Fitting of the five highest ones yields binding constants (as intercept/slope ratios) of $2.4 \times 10^4$, $1.5 \times 10^4$ and $1.3 \times 10^4$ for C1, C2 and C3, respectively (the fitting of C3 data is shown as an inset to Fig. 3c). On the other hand, data at low added amounts of curcuminoids, that are less affected by inner-filter effects, can be analyzed without the above assumption on the free-ligand concentration using the more complex, but still tractable, Eq. (3) in Section 2.4. Non-linear fitting was performed on corrected intensities of samples having absorbances lower than about 0.4 (data not shown). The $K$ values thus obtained were $2 \times 10^4$, $2 \times 10^4$ and $3 \times 10^4$ for C1, C2 and C3, respectively. These results are associated with hardly quantifiable confidence ranges. The first two values are consistent with those obtained from analysis of the five highest-concentration data; for C3, the value is doubled. This confirms the larger uncertainty on C3 data. Overall, however, we believe the results obtained for C1 and C2 from fluorescence enhancement upon complexation with BSA, which are 2 to 5 times larger than those derived from protein-fluorescence quenching, to be definitely more reliable. For C3, from the latter set of experimental data we will only keep the order of magnitude estimation of the binding constant with BSA, several units times $10^4$, which is comparable with those of C1 and C2. These values are well within the range reported for binding constants of curcumin with BSA and HSA, thus confirming the conclusion drawn from the photophysical data, i.e., that the glycosyl substituents in C1–C3 do not change deeply the interaction pattern of curcuminoids with albumins.

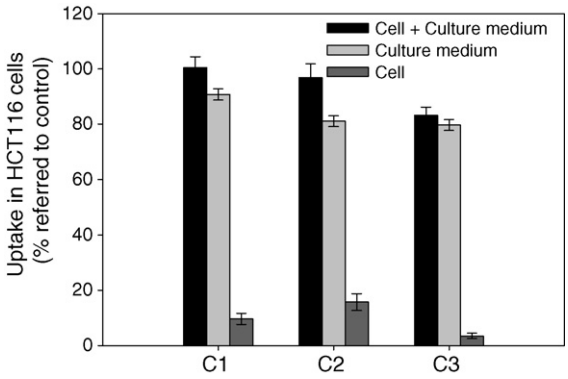


**Fig. 4.** Percentages of C1, C2 and C3 extracted from culture medium and HCT116 cells at 20 μM treatment. All data are normalized to the control and represent means ± SD of three independent experiments.

### 3.3. Distribution in cells monitored by confocal fluorescence microscopy

We have finally exploited the information obtained from the previously described experiments on the environmental sensitivity of curcuminoid fluorescence to try to interpret images of HCT116 cells incubated with compounds C1–C3 obtained with fluorescence confocal microscopy. A preliminary kinetic study of the stability of curcumin and C1–C3 in water has shown that degradation is extremely slow at pH 7 for all glycosylated curcuminoids: the fraction of decomposed compounds was lower than 30% after 8 h, while curcumin already decomposed by 50% in the first hour. We compared the uptake of C1–C3 by HCT116 cells during the course of 24 h treatments by extracting the curcuminoids from both the cells and their culture medium. The percentages of each compound in the cell and culture medium, referred to the specific control solution maintained in the same condition in the culture medium, allowed for a comparison of cellular uptake (Fig. 4). We recovered a large fraction of all curcuminoids, around 80–90%, in the culture medium. While for C1 and C2 the fractions recovered in the cells and in the culture medium summed up to, roughly, unity, for C3 they accounted only for 80% of the control, hinting that this compound had been involved in more efficient metabolic degradation pathways inside the cell. This hypothesis is supported by the observation of a greater cytotoxic activity of C3 with respect to the other

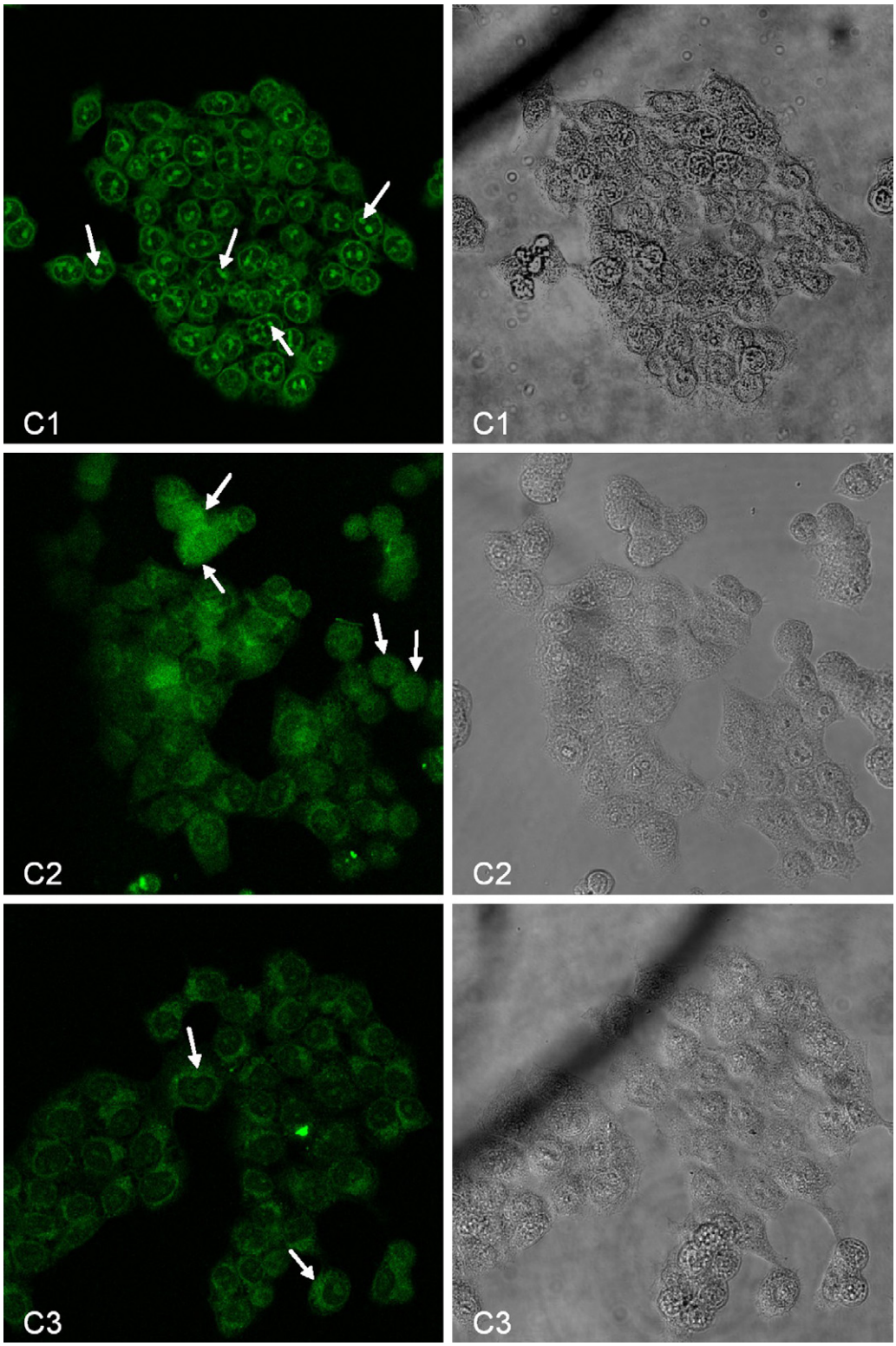


**Fig. 5.** Confocal microscopy analysis of C1, C2 and C3 intracellular distribution in HCT116 cells. Left: confocal fluorescence images; right: phase contrast images. The arrows in each panel indicate nuclear inclusions, pan-cellular and cytoplasmic accumulation of C1, C2 and C3, respectively.

two glycosyl-curcuminoids towards human ovarian carcinoma cell lines [9].

Confocal fluorescence microscopy showed that, although C3 was the best emitting curcuminoid in water and the most uptaken one, it featured a weak emission in cells, mainly from the cytoplasm (Fig. 5, arrows). Again, this points to the existence of intra-cellular processes which lead to partial C3 degradation into non-fluorescent metabolites. A similar intracellular localization was observed for C2, even if some cells showed a pan-cellular (cytoplasmic and nuclear) fluorescence (Fig. 5, arrows). Conversely, C1 was mainly accumulated in the nuclear membranes and strongly emitting small inclusions were observed in the nuclei, suggesting a marked accumulation within nucleoli (Fig. 5, arrows).

## 4. Discussion

The photophysical observations in water and organic media described above, while hinting at a major role of solute–solvent hydrogen bonds involving O atoms of the 3,3′ phenyl substituents in the $3 \times 10^{10}$–$3 \times 10^{11}$ $s^{-1}$ radiationless decays of C1 and C2 in hydrogen-bonding solvents, provide but little new information concerning the slower decay paths, likely characterized by ESIPT at the intramolecularly hydrogen-bonded keto–enol moiety, featured by curcumin and, in non-hydrogen bonding solvents, our curcuminoids: the different substitutions at the $C_3$s and $C_4$s of the phenyl rings cause but a minor modulation of the rates of these paths, as suggested by the $k_{nr}$ values in acetonitrile, $1.2 \times 10^9$ $s^{-1}$ [2] and $2.5 \times 10^9$ $s^{-1}$ [16] for curcumin and $1.2–2.9 \times 10^9$ $s^{-1}$ for C1–C3.

Effects of intermolecular hydrogen bonds on the photophysical properties of various compounds have been known for a long time and have been interpreted in terms of several mechanisms (see e.g., [39–41] and references quoted therein). For example, in planar N-heterocyclic and aromatic carbonyl compounds coupling of close-lying $\pi\pi^*$ and $n\pi^*$ states, which favours, among other processes, radiationless deactivation, may be modulated by changing the relative state energies upon formation of solute–solvent hydrogen bonds that involve the atoms which carry the non-bonding orbitals. Such a 'proximity effect' [42], however, is not likely to account for the observations reported above for the following two reasons: (i) no $n\pi^*$ state lies within 0.4–0.5 eV above the $S_1$ $\pi\pi^*$ state of curcumin even in the gas-phase [24,33]. Polar and protic solvents are expected to further stabilize the latter relative to the former [42] and make the energy gap larger and, correspondingly, the vibronic coupling negligibly small; (ii) this phenomenon assigns a key role to the central carbonyl group, rather than the $OCH_3$/OH ring substituents. To explain the observations, we would then need to make the specious assumption that such substitutions may increase in this order the proneness of the curcuminoid chromophore to undergo proximity effects upon formation of hydrogen bonds with the solvent through the carbonyl O atom(s).

According to a second mechanism, a change in strength, particularly an increase, of intermolecular hydrogen bonds between the ground and excited states may provide a dissipative path for rapid internal conversion to the ground state (see, e.g., [39,43–47] and references quoted therein). The high-energy OH oscillators ($3400\ cm^{-1}$), belonging to either the solvent or the solute, serve as efficient energy acceptors in the radiationless transition. Most of the reported examples of such a mechanism involve alcohols as solvents and, as solutes, carbonyl-containing compounds, such as, e.g., anthraquinones [48], aminoanthraquinones [41,49,50], fluorenone and derivatives [40,43,45,47,51,52], Michler's thione [53], coumarin 102 [46], Nile Red dyes [54], 2-piperidinoanthraquinone [44]. Examples in which N-heterocycles act as hydrogen-bonding acceptors from alcohols are reported as well, but with a change in mechanism which here encompasses an excited-state proton transfer [55]. We are not aware of cases in which this mechanism operates to enhance the radiationless decay of chromophores that form hydrogen bonds with water or alcohols through phenoxyl O atoms. Of some relevance to the case of C1 in protic solvents is the mechanism that underlies fast radiationless deactivation of compounds, such as 7-azaindole, 1-azacarbazole, hydroxyquinolines, 3-hydroxyflavone and others, that can simultaneously act as donors and acceptors in hydrogen bond formation with water or alcohols (see [39] and references quoted therein). In the excited states of these systems, cyclic complexes with water or the alcohol are formed and a concerted double tautomerization coordinate opens up a fast radiationless decay channel.

At present we are unable to say which of these mechanisms may apply to rationalize the unusually fast radiationless decays of C1 in water, methanol and DMSO. The timescale of radiationless decay of C1 in methanol and DMSO, $k_{nr} \sim 3–4 \times 10^{10}$ $s^{-1}$, compares with typical values found for the concerted tautomeric mechanism of pyridylindoles in alcohols, $10^{10}$–$10^{11}$ $s^{-1}$ [39]. Somewhat slower hydrogen-bonding-mediated radiationless decays are reported for fluorenone ($k_{nr} = 5 \times 10^9$ $s^{-1}$ [44]), aminofluorenones ($k_{nr} = 2 \times 10^8$–$1 \times 10^{10}$ $s^{-1}$ [51]), anthraquinones ($k_{nr} = 2–4 \times 10^9$ $s^{-1}$ [48]), aminoanthraquinones ($k_{nr} = 2 \times 10^9$–$2 \times 10^{10}$ $s^{-1}$ [49]) and OH-substituted Nile Red ($k_{nr} = 1 \times 10^8$–$1 \times 10^9$ $s^{-1}$ [54]) in short aliphatic alcohols. Apparently, no kinetic data is available for the same compounds in water and it is therefore not possible to check whether the timescales of these processes may increase by one/two orders of magnitude with respect to those in alcohols, so as to compare with the value found with C1 ($k_{nr} \sim 4 \times 10^{11}$ $s^{-1}$).

A final comment related with mechanistic features concerns the photophysical consequences of the position of the OH substituents: in the case of curcumin, where such groups are bound at $C_{4,4'}$, $k_{nr}$ is larger by only a factor 3–5 in hydrogen-bond accepting solvents (DMSO and dimethylformamide) relative to non-hydrogen bonding acetonitrile [16,17], while for 3,3′-OH-disubstituted C1 such an increase amounts to a factor 15–20 (Table 1). This difference correlates with the larger change in electron density at atoms $C_3$ relative to $C_4$ calculated between the frontier molecular orbitals of curcumin (see Fig. 4 in Ref. [26]) and suggests a correspondingly larger excitation-induced change in hydrogen-bond strengths of C1 with respect to curcumin. An additional explanation for the mentioned difference between C1 and curcumin is related with the different attitudes of the ring substituents to give intramolecular hydrogen bonds: structural calculations show that, in vacuum, the OH and $OCH_3$ ring substituents of curcumin are hydrogen-bonded to each other [24], while the $C_{3,3'}$–OH groups of C1 only weakly interact with the glycosyl groups [56] and should therefore be more apt to establish hydrogen bonds with solvent molecules. Whatever the explanation, however, comparison of the photophysics of C1 with that of curcumin further confirms the central role of hydrogen bonds involving the $C_{3,3'}$–OH groups in the ultrafast radiationless decay of C1 in water.

## 5. Conclusions

Glycosylation has conferred to curcuminoids C1–C3 higher solubility and stability towards degradation in water, thus enabling us to investigate the electronic spectra and photophysics of these compounds in such a biologically relevant solvent. Based on the UV–vis spectra, we conclude these compounds to be fully protonated in water at pH 3 and to equilibrate between the di-keto and the keto–enol forms of the central β-dicarbonyl moiety. The latter form, stabilized by a strong intramolecular hydrogen bond, prevails in all organic solvents, as previously observed with curcumin, and dominates fluorescence emission in all media, including water. The glycosylated curcuminoids C1–C3, which only differ in the 3,3′-phenyl-ring substituents, exhibit a widely differing solvent dependence of photophysical behaviours. While fluorescence quantum yields and $S_1$-state radiationless-decay rates are similar for the three compounds in aprotic organic solvents, and compare with those of curcumin in organic media, formation of solute–solvent hydrogen bonds involving 3,3′-substituents able to act either as acceptors (–$OCH_3$, C2) or as both donors and acceptors (–OH, C1) results in an increase in the radiationless-decay rate constant; this is most pronounced in water where it amounts to more than one and two orders of magnitude for C2 and C1, respectively. No evidence has been observed of any dependence of the $S_1$-state decay rate on intermolecular hydrogen bonds possibly involving the central β-dicarbonyl moiety.

The observed solvent effects suggest that C1 and C2 fluorescence monitoring may be employed to probe the hydrogen-bonding donor/acceptor ability of their microenvironment, including hydrophilic/hydrophobic domains in complex biological systems. Indeed, interaction with bovine serum albumin enhances fluorescence emission from C1 and C2 through a decrease in the radiationless decay rate that is larger for the less emitting compound, C1. Quantum yields remain, however, much smaller than in aprotic solvents. These findings point to a reduced hydrophilic – yet not fully hydrophobic – character of the curcuminoid microenvironment in the complex with BSA. On the other hand, the insensitivity of C3 emission intensity to changes in the medium nature is reproduced in its interaction with BSA. Curcuminoid-BSA binding constants are all in the range few units $\times 10^4$–$10^5$ $M^{-1}$, the same as reported for curcumin. This observation suggests the relevant, hydrophobic curcuminoid/protein interactions to be only little affected by glycosylation.

Finally, the significant differences observed for the three curcuminoids in confocal fluorescence imaging of HCT116 cells, combined with their differences in uptake and cytotoxicity, suggest the apparently small structural differences to actually modulate, besides their fluorescence behaviour, their interactions, localization and fate within living cells.

## Acknowledgements

Bert Vogelstein (Johns Hopkins University School of Medicine, Baltimore, MD) is thanked for generously providing the HCT116 cell line. We thank the "Centro Interdipartimentale Grandi Strumenti (CIGS)" of the University of Modena and Reggio Emilia for making available the Leica DM IRE2 confocal microscope.

## References

[1] H. Hatcher, R. Planalp, J. Cho, F.M. Torti, S.V. Torti, Cell. Mol. Life Sci. 65 (2008) 1631–1652.
[2] L. Nardo, A. Andreoni, M. Bondani, M. Másson, H.H. Tønnesen, J. Photochem. Photobiol. B: Biol. 97 (2009) 77–86.
[3] Y.J. Wang, M.H. Pan, A.L. Cheng, L.I. Lin, Y.S. Ho, C.Y. Hsieh, J.K. Lin, J. Pharm. Biomed. Anal. 15 (1997) 1867–1876.
[4] H.H. Tønnesen, M. Másson, T. Loftsson, Int. J. Pharm. 244 (2002) 127–135.
[5] S. Kumar, U. Narain, S. Tripathi, K. Misra, Bioconjugate Chem. 12 (2001) 464.
[6] W. Shi, S. Dolai, S. Rizk, A. Hussain, H. Tariq, S. Averick, W. L'Amoreaux, A. El Idrissi, P. Banerjee, K. Raja, Org. Lett. 9 (2007) 5461–5464.
[7] B. Arezzini, M. Ferrali, E. Ferrari, R. Grandi, S. Monti, M. Saladini, Eur. J. Inorg. Chem. 3 (2004) 646–652.
[8] E. Ferrari, B. Arezzini, M. Ferrali, S. Lazzari, F. Pignedoli, F. Spagnolo, M. Saladini, BioMetals 22 (2009) 701–710.
[9] E. Ferrari, S. Lazzari, G. Marverti, F. Pignedoli, F. Spagnolo, M. Saladini, Biorg. Med. Chem. 17 (2009) 3043–3052.
[10] A.C. Pulla Reddya, E. Sudharshanb, A.G. Appu Raob, B.R. Lokesha, Lipids 34 (1999) 1025–1029.
[11] A. Kunwar, A. Barik, R. Pandey, K.I. Priyadarsini, Biochim. Biophys. Acta 1760 (2006) 1513–1520.
[12] F. Wang, J. Yang, X. Wu, F. Wang, S. Liu, Anal. Bioanal. Chem. 385 (2006) 139–145.
[13] A. Barik, B. Mishra, A. Kunwar, K.I. Priyadarsini, Chem. Phys. Lett. 436 (2007) 239–243.
[14] A. Barik, K.I. Priyadarsini, H. Mohan, Photochem. Photobiol. 77 (2003) 597–603.
[15] C.F. Chignell, P. Bilskj, K.J. Reszka, A.G. Motten, R.H. Sik, T.A. Dahl, Photochem. Photobiol. 59 (1994) 295–302.
[16] S.M. Khopde, K.I. Priyadarsini, D.K. Palit, T. Mukherjee, Photochem. Photobiol. 72 (2000) 625–631.
[17] L. Nardo, R. Paderno, A. Andreoni, T. Haukvik, M. Màsson, H.H. Tønnesen, Spectroscopy 22 (2008) 187–198.
[18] J. Toullec, in: Z. Rappoport (Ed.), The Chemistry of Enols, John Wiley & Sons, New York, 1990, pp. 323–398.
[19] J.T. Mague, W.L. Alworth, F.L. Payton, Acta Cryst. C60 (2004) o608–o610.
[20] H.H. Tønnesen, J. Karlsen, A. Mostad, U. Pedersen, P.B. Rasmussen, S.-O. Lawesson, Acta Chem. Scand. B 37 (1983) 179–185.
[21] J. Karlsen, A. Mostad, H.H. Tønnesen, Acta Chem. Scand. B 42 (1988) 23–27.
[22] A.M. Anderson, M.S. Mitchell, R.S. Mohan, J. Chem. Educ. 77 (2000) 359–360.
[23] L.R.C. Barclay, M.R. Vinqvist, K. Mukai, H. Goto, Y. Hashimoto, A. Tokunaga, H. Uno, Org. Lett. 2 (2000) 2841–2843.
[24] R. Benassi, E. Ferrari, S. Lazzari, F. Spagnolo, M. Saladini, J. Mol. Struct. 892 (2008) 168–176.
[25] L. Shen, H.-F. Ji, Spectrochim. Acta A 67 (2007) 619–623.
[26] K. Balasubramanian, J. Agric. Food Chem. 54 (2006) 3512–3520.
[27] R. Adhikary, P. Mukherjee, T.W. Kee, J.W. Petrich, J. Phys. Chem. B 113 (2009) 5255–5261.
[28] B.J. Schwartz, L.A. Peteanu, C.B. Harris, J. Phys. Chem. 96 (1992) 3591–3598.
[29] B. Valeur, Molecular Fluorescence, Wiley-VCH, Weinheim, 2002, p. 24.
[30] J.H. Brannon, D. Magde, J. Phys. Chem. 82 (1978) 705–709.
[31] B. Valeur, Molecular Fluorescence, Wiley-VCH, Weinheim, 2002, pp. 339–348.
[32] J.R. Lakowicz, Principles of Fluorescence Spectroscopy, third ed., Springer, New York, 2006, pp. 55–56.
[33] E. Benassi, F. Spagnolo, Theor. Chem. Acc. 124 (2009) 235–250.
[34] B.K. Sahoo, K.S. Ghosh, S. Dasgupta, Biophys. Chem. 132 (2008) 81–88.
[35] S. Formosinho, L.G. Arnaut, J. Photochem. Photobiol. A: Chem. 75 (1993) 21–48.
[36] U. Kragh-Hansen, Pharmacol. Rev. 33 (1981) 17–53.
[37] T. Peters Jr., Adv. Protein Chem. 37 (1985) 161–245.
[38] M.K. Singh, H. Pal, A.S.R. Koti, A.V. Sapre, J. Phys. Chem. A 108 (2004) 1465–1474.
[39] J. Herbich, C.-Y. Hung, R.P. Thummel, J. Waluk, J. Am. Chem. Soc. 118 (1996) 3508–3518.
[40] L. Biczok, T. Berces, H. Inoue, J. Phys. Chem. A 103 (1999) 3837–3842.
[41] A. Morimoto, T. Yatsuhashi, T. Shimada, L. Biczok, D.A. Tryk, H. Inoue, J. Phys. Chem. A 105 (2001) 10488–10496.
[42] E.C. Lim, J. Phys. Chem. 90 (1986) 6770–6777.
[43] L. Biczok, T. Berces, H. Linschitz, J. Am. Chem. Soc. 119 (1997) 11071–11077.
[44] A. Morimoto, T. Yatsuhashi, T. Shimada, S. Kumazaki, K. Yoshihara, H. Inoue, J. Phys. Chem. A 105 (2001) 8840–8849.
[45] V. Samant, A.K. Singh, G. Ramakrishna, H.N. Ghosh, T.K. Ghanty, D.K. Palit, J. Phys. Chem. A 109 (2005) 8693–8704.
[46] G.-J. Zhao, K.-L. Han, J. Phys. Chem. A 111 (2007) 2469–2474.
[47] G.-J. Zhao, K.-L. Han, J. Phys. Chem. A 111 (2007) 9218–9223.
[48] S.R. Flom, P.F. Barbara, J. Phys. Chem. A 89 (1985) 4489–4494.
[49] H. Inoue, M. Hida, N. Nakashima, K. Yoshihara, J. Phys. Chem. A 86 (1982) 3184–3188.
[50] T. Yatsuhashi, H. Inoue, J. Phys. Chem. A 101 (1997) 8166–8173.
[51] T. Yatsuhashi, Y. Nakajima, T. Shimada, H. Inoue, J. Phys. Chem. A 102 (1998) 3018–3024.
[52] T. Yatsuhashi, Y. Nakajima, T. Shimada, H. Tachibana, H. Inoue, J. Phys. Chem. A 102 (1998) 8657–8663.
[53] J.A. Mondal, H.N. Ghosh, T. Mukherjee, D.K. Palit, J. Phys. Chem. A 110 (2006) 12103–12112.
[54] K. Nagy, S. Göktürk, L. Biczok, J. Phys. Chem. A 107 (2003) 8784–8790.
[55] T.A. Fayed, S.E.-D.H. Etaiw, S. Landgraf, G. Grampp, Photochem. Photobiol. Sci. 2 (2003) 376–380.
[56] R. Benassi, E. Ferrari, S. Lazzari, F. Pignedoli, F. Spagnolo, M. Saladini, submitted for publication.